

# A spatial model for rare binary events

July 28, 2016

## 1 Introduction

The goal in binary regression is to relate a latent variable to a response using a link function. Two common examples of binary regression include logistic regression and probit regression (Agresti, 2003). The link functions for logistic and probit regression are symmetric, so they may not be well-suited for binary data with very few ones. An asymmetric alternative to these link functions is the complementary log-log (cloglog) link function. More recently, Wang and Dey (2010) introduced the generalized extreme value (GEV) link function for rare binary data (a review is given in Appendix A.1). The GEV link function introduces a new shape parameter to the link function that controls the degree of asymmetry. The cloglog link is a special case of the GEV link function when the shape parameter is 0. Although this link was selected due to its ability to handle asymmetry, the GEV distribution is one of the primary distributions used for modeling extremes (Coles, 2001). Because extreme events are rare, it is therefore reasonable to use similar methods when analyzing rare binary data.

Most popular methods for spatial binary data propose a latent continuous spatial process with the binary response determined by whether the latent process exceeds a threshold (De Oliveira, 2000; Diggle and Ribeiro, 2007). In the hierarchical framework, spatial dependence is typically modeled with an underlying latent Gaussian process, and conditioned on this process, observations are independent. For large datasets, low-rank models can be used to ease the computational burden (Finley et al., 2015). A Gaussian process is not appropriate for modeling extremal dependence in a distribution because there is no asymptotic dependence except in the case of perfect dependence. This lack of asymptotic dependence leads to an underestimation of probability that two observations will jointly exceed a high threshold.

We propose using a latent max-stable process (de Haan, 1984) because it allows for asymptotic dependence. The max-stable process arises as the limit of the location-wise maximum of infinitely many spatial processes. Max-stable processes are extremely flexible, but are often challenging to work with in high dimensions (Wadsworth and Tawn, 2014; Thibaud and Opitz, 2015). To address this challenge, methods have been proposed that implement composite likelihood techniques for max-stable processes (Padoan et al., 2010; Genton et al., 2011; Huser and Davison, 2014). Composite likelihoods have been used to model binary spatial data (Heagerty and Lele, 1998), but this is not using max-stable processes. As an alternative to these composite approaches, Reich and Shaby (2012) present a hierarchical model that implements a low-rank representation for a max-stable process. We chose to use this low-rank representation for our rare binary spatial regression model.

Paragraph outlining the structure of the paper

## 2 Spatial dependence for binary regression

Let  $Y(\mathbf{s})$  be the binary response at spatial location  $\mathbf{s}$  in a spatial domain of interest  $\mathcal{D} \in \mathcal{R}^2$ . We assume  $Y(\mathbf{s}) = I[Z(\mathbf{s}) > 0]$  where  $Z(\mathbf{s})$  is a latent continuous max-stable process. The marginal distribution of  $Z(\mathbf{s})$  at site  $\mathbf{s}$  is GEV with location  $\mathbf{X}(\mathbf{s})^\top \boldsymbol{\beta}$ , scale  $\sigma > 0$ , and shape  $\xi$ , where  $\mathbf{X}(\mathbf{s})$  is a  $p$ -vector of spatial covariates at site  $\mathbf{s}$  and  $\boldsymbol{\beta}$  is a  $p$ -vector of regression coefficients. We set  $\sigma = 1$  for identifiability because only the sign and not the scale of  $Z$  affects  $Y$ . If  $\mathbf{X}(\mathbf{s})^\top \boldsymbol{\beta} = \mu$  for all  $\mathbf{s}$ , then  $P(Y = 1)$  is the same for all observations, and the two parameters  $\mu$  and  $\xi$  are not individually identifiable, so when there are no covariates, we fix  $\xi = 0$ . Although  $\boldsymbol{\beta}$  and  $\xi$  could be permitted to vary across space, we assume that they are constant across  $\mathcal{D}$ . At spatial location  $\mathbf{s}$ , the marginal distribution (over  $Z(\mathbf{s})$ ) is  $P[Y(\mathbf{s}) = 1] = 1 - \exp\left[-\frac{1}{z(\mathbf{s})}\right]$  where  $z(\mathbf{s}) = [1 - \xi \mathbf{X}(\mathbf{s})^\top \boldsymbol{\beta}]^{1/\xi}$ . This is the same as the marginal distribution given by Wang and Dey (2010).

45 For a finite collection of locations  $\mathbf{s}_1, \dots, \mathbf{s}_n$ , denote the vector of observations  $\mathbf{Y} = [Y(\mathbf{s}_1), \dots, Y(\mathbf{s}_n)]^T$ .  
 46 The spatial dependence of  $\mathbf{Y}$  is determined by the joint distribution of  $\mathbf{Z} = [Z(\mathbf{s}_1), \dots, Z(\mathbf{s}_n)]^T$ . To incor-  
 47 porate spatial dependence, we consider the hierarchical representation of the max-stable process proposed  
 48 in Reich and Shaby (2012). Consider a set of positive stable random effect  $A_1, \dots, A_L \stackrel{iid}{\sim} \text{PS}(\alpha)$  associated  
 49 with spatial knots  $\mathbf{v}_1, \dots, \mathbf{v}_L \in \mathcal{R}^2$ . The hierarchical model is given by

$$\mathbf{Z}(\mathbf{s}_i) | A_1, \dots, A_L \stackrel{indep}{\sim} \text{GEV}[\mathbf{X}(\mathbf{s}_i)^\top \boldsymbol{\beta} + \theta(\mathbf{s}_i), \alpha \theta(\mathbf{s}_i), \xi \alpha] \quad \text{and} \quad \theta(\mathbf{s}_i) = \left[ \sum_{l=1}^L A_l w_l(\mathbf{s}_i)^{1/\alpha} \right]^\alpha \quad (1)$$

50 where  $w_l(\mathbf{s}_i) > 0$  are a set of  $L$  weights that vary smoothly across space and satisfy  $\sum_{l=1}^L w_l(\mathbf{s}) = 1$  for all  
 51  $\mathbf{s}$ , and  $\alpha \in (0, 1)$  determines the strength of dependence, with  $\alpha$  near zero giving strong dependence and  
 52  $\alpha = 1$  giving joint independence.

53 Because the latent  $\mathbf{Z}(\mathbf{s})$  are independent given the random effects  $\theta(\mathbf{s})$ , the binary responses are also  
 54 conditionally independent. This leads to the tractable likelihood

$$Y(\mathbf{s}_i) | A_1, \dots, A_L \stackrel{indep}{\sim} \text{Bern}[\pi(\mathbf{s}_i)] \quad (2)$$

55 where

$$\pi(\mathbf{s}_i) = 1 - \exp \left\{ - \sum_{l=1}^L A_l \left( \frac{w_l(\mathbf{s}_i)}{z(\mathbf{s}_i)} \right)^{1/\alpha} \right\}. \quad (3)$$

56 Marginally over the  $A_l$ , this gives

$$Z(\mathbf{s}) \sim \text{GEV}(\mathbf{X}(\mathbf{s})^\top \boldsymbol{\beta}, 1, \xi), \quad (4)$$

57 and thus  $P[Y(\mathbf{s}) = 1] = 1 - \exp \left\{ -\frac{1}{z(\mathbf{s})} \right\}$  where  $z(\mathbf{s}) = [1 - \xi \mathbf{X}(\mathbf{s})\boldsymbol{\beta}]^{1/\xi}$ .

58 Many weight functions are possible, but the weights must be constrained so that  $\sum_{l=1}^L w_l(\mathbf{s}_i) = 1$  for  
 59  $i = 1, \dots, n$  to preserve the marginal GEV distribution. For example, Reich and Shaby (2012) take the  
 60 weights to be scaled Gaussian kernels with knots  $\mathbf{v}_l$ ,

$$w_l(\mathbf{s}_i) = \frac{\exp \left[ -0.5 (\|\mathbf{s}_i - \mathbf{v}_l\|/\rho)^2 \right]}{\sum_{j=1}^L \exp \left[ -0.5 (\|\mathbf{s}_i - \mathbf{v}_j\|/\rho)^2 \right]} \quad (5)$$

61 where  $\|\mathbf{s}_i - \mathbf{v}_l\|$  is the distance between site  $\mathbf{s}_i$  and knot  $\mathbf{v}_l$ , and the kernel bandwidth  $\rho > 0$  determines the  
 62 spatial range of the dependence, with large  $\rho$  giving long-range dependence and vice versa.

63 After marginalizing out the positive stable random effects, the joint distribution of  $\mathbf{Z}$  is

$$G(\mathbf{z}) = P[Z(\mathbf{s}_1) < z(\mathbf{s}_1), \dots, Z(\mathbf{s}_n) < z(\mathbf{s}_n)] = \exp \left\{ -\sum_{l=1}^L \left[ \sum_{i=1}^n \left( \frac{w_l(\mathbf{s}_i)}{z(\mathbf{s}_i)} \right)^{1/\alpha} \right]^\alpha \right\}, \quad (6)$$

64 where  $G(\cdot)$  is the CDF of a multivariate GEV distribution. This is a special case of the multivariate GEV  
 65 distribution with asymmetric Laplace dependence function (Tawn, 1990).

### 66 **3 Joint distribution**

67 We give an exact expression in the case where there are only two spatial locations which is useful for  
 68 constructing a pairwise composite likelihood (Padoan et al., 2010) and studying spatial dependence. When

69  $n = 2$ , the probability mass function is given by

$$P[Y(\mathbf{s}_i) = y_i, Y(\mathbf{s}_j) = y_j] = \begin{cases} \varphi(\mathbf{z}) & y_i = 0, y_j = 0 \\ \exp\left\{-\frac{1}{z(\mathbf{s}_i)}\right\} - \varphi(\mathbf{z}), & y_i = 1, y_j = 0 \\ \exp\left\{-\frac{1}{z(\mathbf{s}_j)}\right\} - \varphi(\mathbf{z}), & y_i = 0, y_j = 1 \\ 1 - \exp\left\{-\frac{1}{z(\mathbf{s}_i)}\right\} - \exp\left\{-\frac{1}{z(\mathbf{s}_j)}\right\} + \varphi(\mathbf{z}), & y_i = 1, y_j = 1 \end{cases} \quad (7)$$

70 where  $\varphi(\mathbf{z}) = \exp\left\{-\sum_{l=1}^L \left[\left(\frac{w_l(\mathbf{s}_i)}{z(\mathbf{s}_i)}\right)^{1/\alpha} + \left(\frac{w_l(\mathbf{s}_j)}{z(\mathbf{s}_j)}\right)^{1/\alpha}\right]^\alpha\right\}$ . For more than two locations, we are also  
 71 able to compute the exact likelihood when the  $n$  is large but the number of events  $K = \sum_{i=1}^n Y(\mathbf{s}_i)$  is small,  
 72 as might be expected for very rare events, see Appendix A.2.

## 73 4 Quantifying spatial dependence

74 Assume that  $Z_1$  and  $Z_2$  are both  $\text{GEV}(\beta, 1, 1)$  so that  $P(Y_i = 1)$  decreases to zero as  $\beta$  increases. A common  
 75 measure of dependence between binary variables is Cohen's Kappa (Cohen, 1960),

$$\kappa(\beta) = \frac{P_A - P_E}{1 - P_E} \quad (8)$$

76 where  $P_A$  is the joint probability of agreement  $P(Y_1 = Y_2)$  and  $P_E$  is the joint probability of agreement  
 77 under an assumption of independence  $P(Y_i = 1)^2 + P(Y_i = 0)^2$ . For the spatial model,

$$P_A(\beta) = 1 - 2 \exp\left\{-\frac{1}{\beta}\right\} + 2 \exp\left\{-\frac{\vartheta(\mathbf{s}_1, \mathbf{s}_2)}{\beta}\right\}$$

$$P_E(\beta) = 1 - 2 \exp\left\{-\frac{1}{\beta}\right\} + 2 \exp\left\{-\frac{2}{\beta}\right\},$$

78 and

$$\kappa(\beta) = \frac{P_A(\beta) - P_E(\beta)}{1 - P_E(\beta)} = \frac{\exp\left\{-\frac{\vartheta(\mathbf{s}_1, \mathbf{s}_2)-1}{\beta}\right\} - \exp\left\{-\frac{1}{\beta}\right\}}{1 - \exp\left\{-\frac{1}{\beta}\right\}} \quad (9)$$

79 where  $\vartheta(\mathbf{s}_i, \mathbf{s}_j) = \sum_{l=1}^L [w_l(\mathbf{s}_i)^{1/\alpha} + w_l(\mathbf{s}_j)^{1/\alpha}]^\alpha$  is the pairwise extremal coefficient given by Reich and  
 80 Shaby (2012). To measure extremal dependence, let  $\beta \rightarrow \infty$  so that events are increasingly rare. Then,

$$\kappa = \lim_{\beta \rightarrow \infty} \kappa(\beta) = 2 - \vartheta(\mathbf{s}_1, \mathbf{s}_2) \quad (10)$$

81 which is the same as the  $\chi$  statistic of Coles (2001), a commonly used measure of extremal dependence.

## 82 5 Computation

83 For small  $K$ , we can evaluate the likelihood directly. When  $K$  is large, we use Markov chain Monte  
 84 Carlo (MCMC) methods with the random effects model to explore the posterior distribution. To overcome  
 85 challenges with evaluating the positive stable density, we follow Reich and Shaby (2012) and introduce a  
 86 set of auxiliary variables  $B_1, \dots, B_L$  following the auxiliary variable technique of Stephenson (2009) (for  
 87 more details, see Appendix A.3 of Reich and Shaby (2012)). So, the hierarchical model is given by

$$\begin{aligned} Y(\mathbf{s}_i) | \pi(\mathbf{s}_i) &\overset{indep}{\sim} \text{Bern}[\pi(\mathbf{s}_i)] \\ \pi(\mathbf{s}_i) &= 1 - \exp\left\{-\sum_{l=1}^L A_l \left(\frac{w_l(\mathbf{s}_i)}{z(\mathbf{s}_i)}\right)^{1/\alpha}\right\} \\ A_l &\sim \text{PS}(\alpha) \end{aligned} \quad (11)$$

with priors  $\beta \sim N(\mathbf{0}, \sigma_\beta^2 \mathbf{I}_p)$ ,  $\xi \sim N(0, \sigma_\xi^2)$ ,  $\rho \sim \text{Unif}(\rho_l, \rho_u)$ , and  $\alpha \sim \text{Beta}(a_\alpha, b_\alpha)$ . The model parameters are updated using Metropolis Hastings (MH) update steps, and the random effects  $A_1, \dots, A_L$ , and auxiliary variables  $B_1, \dots, B_L$  are updated using Hamiltonian Monte Carlo (HMC) update steps. The code for this is available online through <https://github.com/sammorris81/rare-binary>.

## 6 Simulation study

For our simulation study, we generate  $n_m = 50$  datasets under 12 different simulation settings to explore the impact of sample size, sampling technique, and misspecification of link function. We generate data assuming three possible types of underlying process. For each of the underlying processes, we generate complete datasets on a  $100 \times 100$  rectangular grid of  $n = 10,000$  locations. If a dataset is generated with  $K < 100$  or  $K > 700$ , it is discarded and a new dataset is generated. For model fitting, we select a subsample and use the remaining sites to evaluate predictive performance.

### 6.1 Latent processes

The first process is a latent max-stable process that uses the GEV link described in (1) with knots on a  $50 \times 50$  regularly spaced grid on  $[0, 1] \times [0, 1]$ . For this process, we set  $\alpha = 0.35$ ,  $\rho = 0.1$ , and  $\beta_0 \approx 2.97$  which gives  $K = 500$ , on average. Because there are no covariates, we set  $\xi = 0$ . We then set  $Y(\mathbf{s}) = I[Z(\mathbf{s}) > 0]$ .

For the second process, we generate a latent variable from a spatial Gaussian process with a mean of  $\text{logit}(0.05) \approx -2.94$  and an exponential covariance given by

$$\text{cov}(\mathbf{s}_1, \mathbf{s}_2) = \tau_{\text{Gau}}^2 \exp \left\{ -\frac{\|\mathbf{s}_1 - \mathbf{s}_2\|}{\rho_{\text{Gau}}} \right\} \quad (12)$$

where  $\tau_{\text{Gau}} = 10$  and  $\rho_{\text{Gau}} = 0.1$ . Finally, we generate  $Y(\mathbf{s}_i) \stackrel{\text{ind}}{\sim} \text{Bern}[\pi(\mathbf{s}_i)]$  where  $\pi(\mathbf{s}_i) = \frac{\exp\{z(\mathbf{s}_i)\}}{1 + \exp\{z(\mathbf{s}_i)\}}$

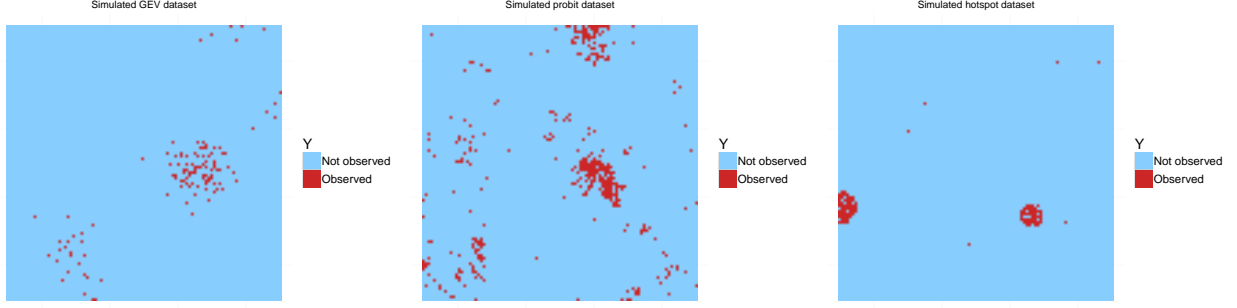


Figure 1: One simulated dataset from spatial GEV (left), spatial logistic (center), and hotspot (right).

For the third process, we generate data using a hotspot method. For this process, we first generate hotspots throughout the space. Let  $n_{\text{hs}}$  be the number of hotspots in the space. Then  $n_{\text{hs}} - 1 \sim \text{Poisson}(2)$ . This generation scheme ensures that every dataset has at least one hotspot. We generate the hotspot locations  $\mathbf{h}_1, \dots, \mathbf{h}_{n_{\text{hs}}} \sim \text{Unif}(0, 1)^2$ . Let  $B_h$  be a circle of radius of radius  $r_h$  around hotspot  $h = 1, \dots, n_{\text{hs}}$ . The  $r_h$  differ for each hotspot and are generated i.i.d. from a  $\text{Unif}(0.03, 0.08)$  distribution. We set  $P[Y(\mathbf{s}_i) = 1] = 0.85$  for all  $\mathbf{s}_i$  in  $B_h$ , and  $P[Y(\mathbf{s}_i)] = 0.0005$  for all  $\mathbf{s}_i$  outside of  $B_h$ . These settings are selected to give an average of approximately  $K = 500$  for the datasets. Figure 1 gives an example dataset from each of the data settings.

## 6.2 Methods

For each dataset, we fit the model using three different models, the proposed spatial GEV model, a spatial probit model, and a spatial logistic model. Logistic and probit methods represent two of the more common spatial techniques for binary data, we chose to compare our method to them. One way these methods differ from our proposed method is that they assume the underlying process is Gaussian. In this case, we assume



119 that  $Z(\mathbf{s})$  follows a Gaussian process with mean  $\mathbf{X}(\mathbf{s})^\top \boldsymbol{\beta}$ . The marginal distributions are given by

$$P[Y(\mathbf{s}) = 1] = \begin{cases} \frac{\exp[\mathbf{X}^\top(\mathbf{s})\boldsymbol{\beta} + \mathbf{W}(\mathbf{s})\boldsymbol{\epsilon}]}{1 + \exp[\mathbf{X}^\top(\mathbf{s})\boldsymbol{\beta} + \mathbf{W}(\mathbf{s})\boldsymbol{\epsilon}]}, & \text{logistic} \\ \Phi[\mathbf{X}^\top\boldsymbol{\beta}(\mathbf{s}) + \mathbf{W}(\mathbf{s})\boldsymbol{\epsilon}], & \text{probit} \end{cases} \quad (13)$$

120 where  $\boldsymbol{\epsilon} \sim N(\mathbf{0}, \tau_L^2 \mathbf{I}_L)$  are Gaussian random effects at the knot locations, and  $\mathbf{W}(\mathbf{s})$  are a set of  $L$  basis  
 121 functions given to recreate the Gaussian process at all sites. We use our own code for the spatial probit  
 122 model, but we use the `spGLM` function in the `spBayes` package (Finley et al., 2015) to fit the spatial  
 123 logistic model. For the probit model, we use

$$\mathbf{W}_l(\mathbf{s}_i) = \frac{\exp[-(\|\mathbf{s}_i - \mathbf{v}_l\|/\rho)^2]}{\sqrt{\sum_{j=1}^L \exp[-(\|\mathbf{s}_i - \mathbf{v}_j\|/\rho)^2]^2}}. \quad (14)$$

124 For the logistic model, the  $\mathbf{W}_l(\mathbf{s}_i)$  are the default implementation from the `spGLM`. **Timings**

### 125 6.3 Sampling technique

126 We subsample the generated data using  $n_s = 100, 250$  initial locations for two different sampling designs.  
 127 The first is a two-stage spatially-adaptive cluster technique (CLU) taken from Pacifici et al. (2016). In this  
 128 design, if an initial location is occupied, we also include the four rook neighbor (north, east, south, and west)  
 129 sites in the sample. For the second design, we use a simple random sample (SRS) with the same number of  
 130 sites included in the cluster sample. For the GEV setting, when  $n_s = 100$ , there are on average 117 sites  
 131 and at most 142 sites in a sample, and when  $n_s = 250$ , there are on average 286 sites and at most 332 sites  
 132 in a sample. For the logistic setting, when  $n_s = 100$ , there are on average 118 sites and at most 147 sites  
 133 in a sample, and when  $n_s = 250$ , there are on average 290 sites and at most 330 sites in a sample. For the  
 134 hotspot setting, when  $n_s = 100$ , there are on average 110 sites and at most 128 sites in a sample, and when

135  $n_s = 250$ , there are on average 275 sites and at most 306 sites in a sample.

## 136 6.4 Priors

137 For all models, we only include an intercept term  $\beta_0$  in the model, and the prior for the intercept is  
138  $\beta_0 \sim N(0, 10)$ . Additionally, for all models, the prior for the bandwidth is  $\rho \sim \text{Unif}(0.001, 1)$ . This lower  
139 bound is selected because it is half of the distance between the rook neighbors of the knots. For the GEV  
140 method, the prior for the spatial dependence parameter is  $\alpha \sim \text{Beta}(2, 5)$ . We select this prior because it  
141 gives greater weight to  $\alpha < 0.5$ , which is the point at which spatial dependence becomes fairly weak, but  
142 also avoids values below 0.1 which can lead to numerical problems. We fix  $\xi = 0$  because we do not include  
143 any covariates. For both the spatial probit and logistic models, the prior on the variance term for the random  
144 effects is  $\text{IG}(0.1, 0.1)$  where  $\text{IG}(\cdot)$  is an Inverse Gamma distribution. For all models, we run the MCMC  
145 sampler for 25,000 iterations with a burn-in period of 20,000 iterations. Convergence is assessed through  
146 visual inspection of traceplots.

## 147 6.5 Model comparisons

148 For each dataset, we fit the model using the  $n_s$  observations as a training set, and validate the model's  
149 predictive power at the remaining grid points. Let  $\mathbf{s}_j^*$  be the  $j$ th site in the validation set. To obtain the  
150 posterior predictive distribution, at each iteration of the MCMC, we generate a spatial field of zeros and  
151 ones at the validation locations. I plan to update this if we have time to rerun the computing. At the moment,  
152 I'm trying to get new results for EBF because of the error I found. Then to obtain  $\hat{P}[Y(\mathbf{s}_j^*) = 1]$ , we take the  
153 average of the posterior distribution for each  $j$ . We consider a few different metrics for comparing model  
154 performance. One score is the Brier scores (Gneiting and Raftery, 2007, BS). The Brier score for predicting  
155 an occurrence at site  $\mathbf{s}$  is given by  $\{I[Y(\mathbf{s}) = 1] - \hat{P}[Y(\mathbf{s}) = 1]\}^2$  where  $I[Y(\mathbf{s}) = 1]$  is an indicator function

Table 1: Brier scores (SE) and AUROC (SE) for GEV, Probit, and Logistic methods from the simulation study.

Setting	$n$	Sample Type	BS			AUROC		
			GEV	Probit	Logistic	GEV	Probit	Logistic
GEV	100	CLU						
		SRS						
	250	CLU						
		SRS						
Probit	100	CLU						
		SRS						
	250	CLU						
		SRS						
Hotspot	100	CLU						
		SRS						
	250	CLU						
		SRS						

indicating that an event occurred at site  $s$ . We average the Brier scores over all test sites, and a lower score indicates a better fit. We also consider the receiver operating characteristic (ROC) curve, and the area under the ROC curve (AUROC) for the different methods and settings. The ROC curve and AUROC are obtained via the `ROCR` (Sing et al., 2005) package in R (R Core Team, 2016). We then average AUCs across all datasets for each method and setting to obtain a single AUC for each combination of method and setting.

## 6.6 Results

Needs updating

Table 2 gives the Brier scores and AUC for each of the methods. In Figure 6 – Figure 4, for each setting we present the vertically averaged ROC curve for each simulation method.

## 7 Data analysis

Needs updating

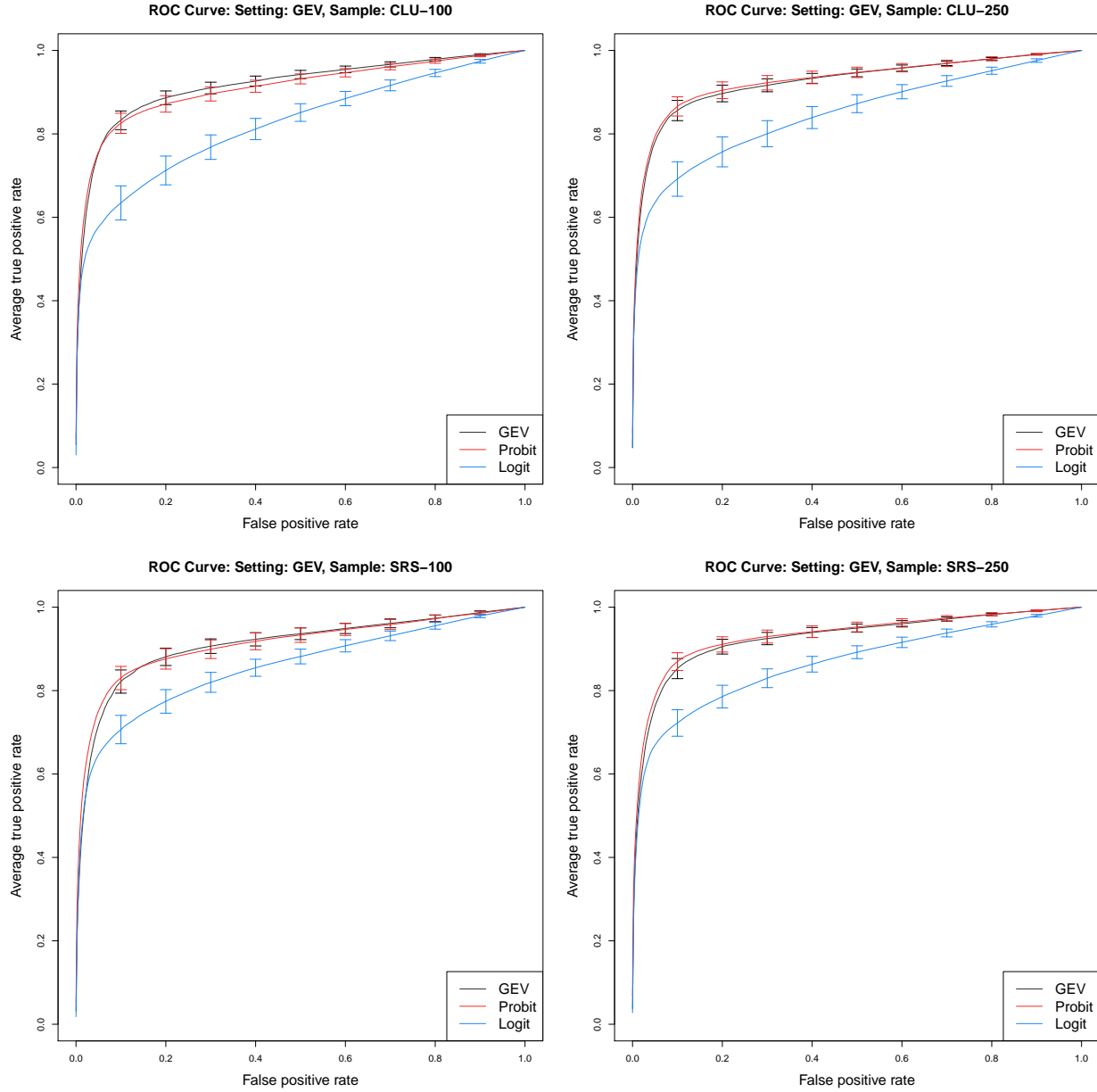


Figure 2: Vertically averaged ROC curves for GEV simulation setting.

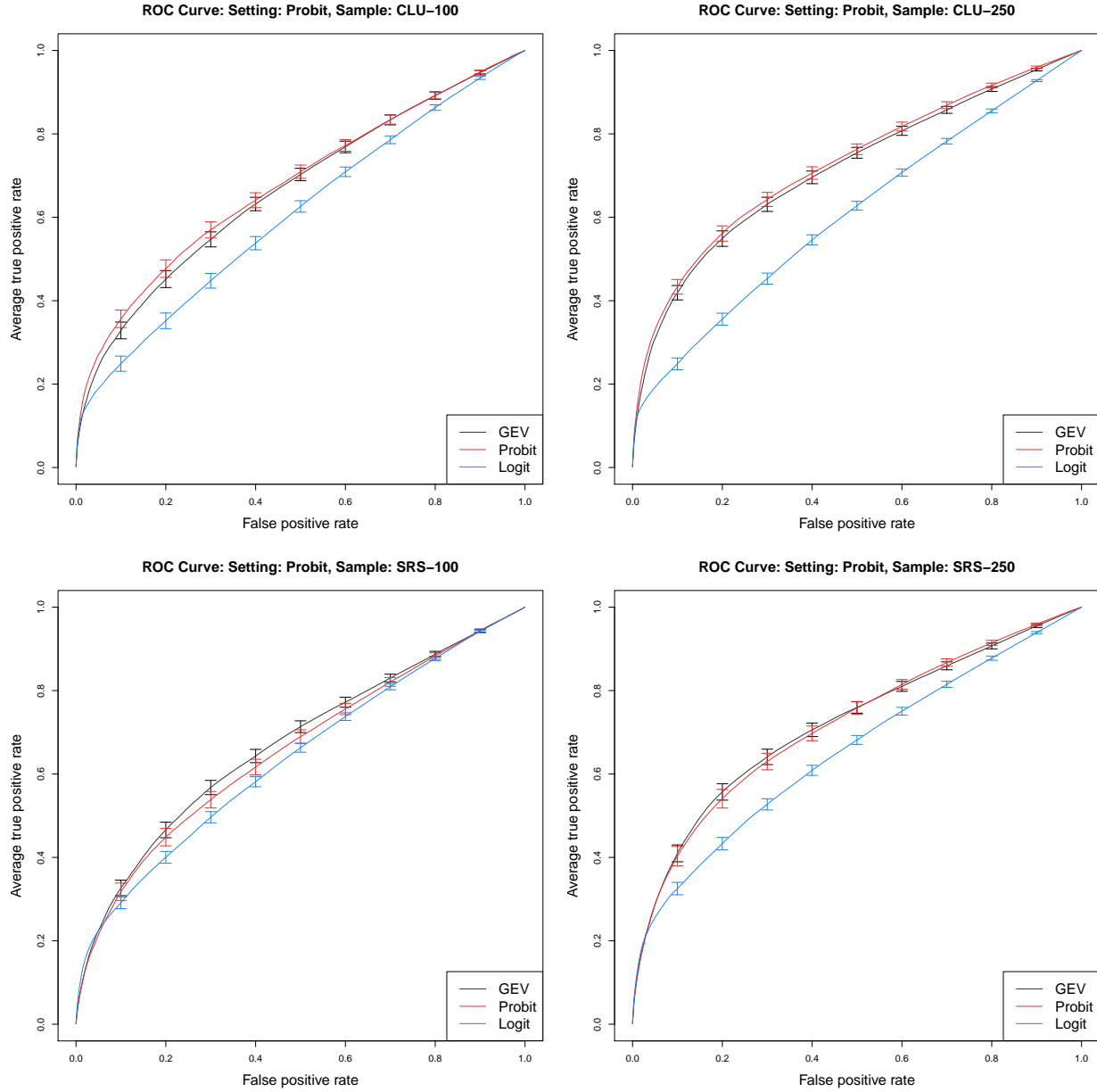


Figure 3: Vertically averaged ROC curves for probit simulation setting.

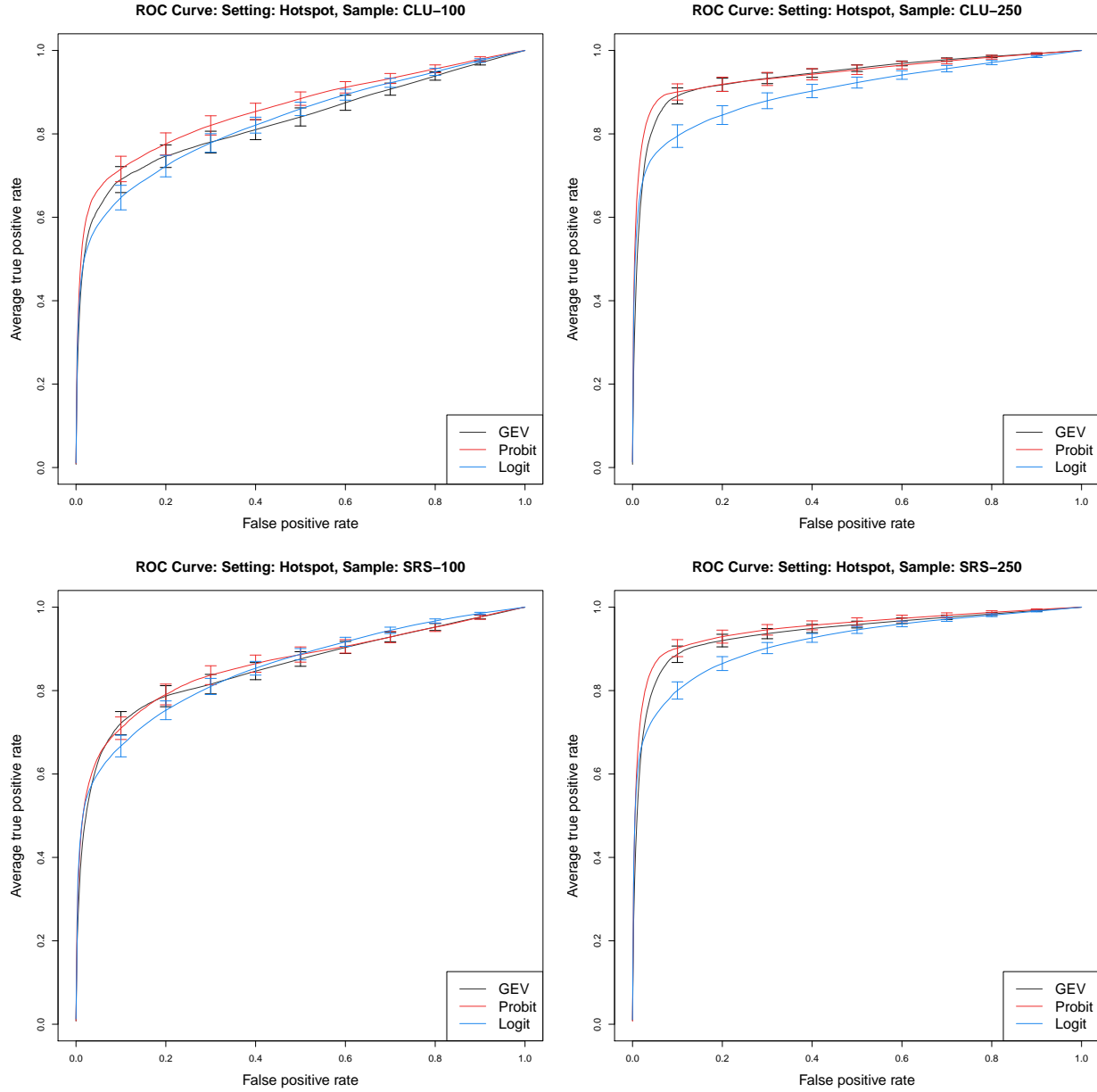


Figure 4: Vertically averaged ROC curves for hotpost simulation setting.

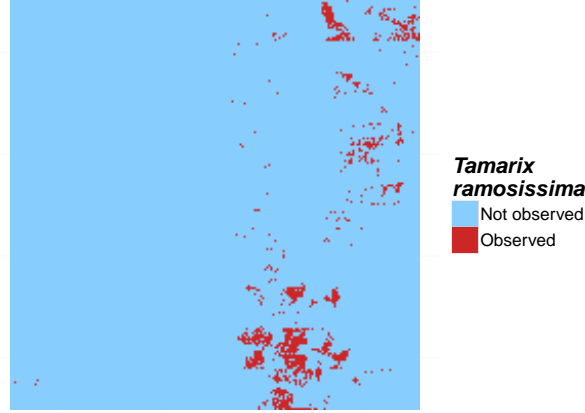


Figure 5: True occupancy of *Tamarix ramosissima* from a 1-km<sup>2</sup> study region of PR China.

We compare our method to the spatial probit and logit for mapping the probability of the occurrence of *Tamarix ramosissima*, a plant species, for a 1-km<sup>2</sup> study region of PR China (Smith et al., 2012). The Chinese Academy of Forestry conducted a full census of the area, and the true occupancy of the species are plotted in Figure 5. The region is split into 10-m  $\times$  10-m grid cells, and *Tamarix ramosissima* can be found in approximately 6% of the grid cells.

## 7.1 Methods

For the data analysis, we generate 100 subsamples using the CLU and SRS sampling methods with  $n_s = 100$  and  $n_s = 250$  initial locations. For each subsample, we fit the spatial GEV, spatial probit, and spatial logistic models. Knot placement, prior distributions, and MCMC details for the data analysis are the same as the simulation study. To compare models, we use similar metrics as in the simulation study, but we average the metrics over subsamples.

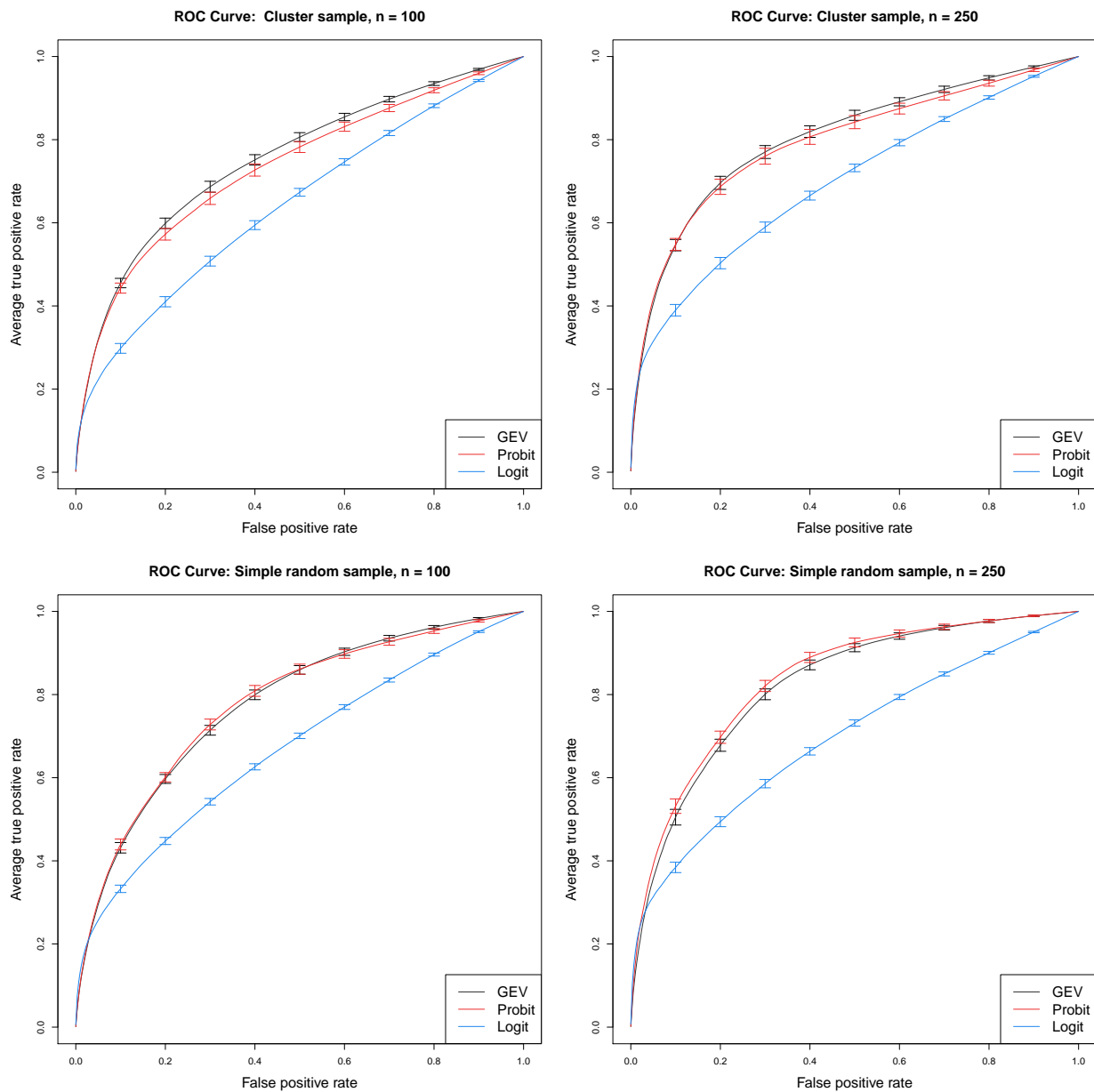


Figure 6: Vertically averaged ROC curves for *Tamarix ramosissima*.



Table 2: Brier scores (SE) and AUROC (SE) for GEV, Probit, and Logistic methods for *Tamarix ramosissima*.

$n$	Sample Type	BS			AUROC		
		GEV	Probit	Logistic	GEV	Probit	Logistic
100	CLU						
	SRS						
250	CLU						
	SRS						

## 7.2 Results

## 8 Conclusions

## Acknowledgments

## A Appendices

### A.1 Binary regression using the GEV link

Here, we provide a brief review of the the GEV link of Wang and Dey (2010). Let  $Y_i \in \{0, 1\}$ ,  $i = 1, \dots, n$  be a collection of i.i.d. binary responses. It is assumed that  $Y_i = I(z_i > 0)$  where  $I(\cdot)$  is an indicator function,  $z_i = [1 - \xi \mathbf{X}_i \boldsymbol{\beta}]^{1/\xi}$  is a latent variable following a  $\text{GEV}(1, 1, 1)$  distribution,  $\mathbf{X}_i$  is the associated  $p$ -vector of covariates with first element equal to one for the intercept, and  $\boldsymbol{\beta}$  is a  $p$ -vector of regression coefficients. Then,  $Y_i \stackrel{\text{ind}}{\sim} \text{Bern}(\pi_i)$  where  $\pi_i = 1 - \exp\left(-\frac{1}{z_i}\right)$ .

### A.2 Derivation of the likelihood

We use the hierarchical max-stable spatial model given by Reich and Shaby (2012). If at each margin,  $Z_i \sim \text{GEV}(1, 1, 1)$ , then  $Z_i | \theta_i \stackrel{\text{indep}}{\sim} \text{GEV}(\theta, \alpha\theta, \alpha)$ . We reorder the data such that  $Y_1 = \dots = Y_K = 1$ , and  $Y_{K+1} = \dots = Y_n = 0$ . Then the joint likelihood conditional on the random effect  $\theta$  is

$$\begin{aligned}
P(Y_1 = y_1, \dots, Y_n = y_n) &= \prod_{i \leq K} \left\{ 1 - \exp \left[ - \left( \frac{\theta_i}{z_i} \right)^{1/\alpha} \right] \right\} \prod_{i > K} \exp \left[ - \left( \frac{\theta_i}{z_i} \right)^{1/\alpha} \right] \\
&= \exp \left[ - \sum_{i=K+1}^n \left( \frac{\theta_i}{z_i} \right)^{1/\alpha} \right] - \exp \left[ - \sum_{i=K+1}^n \left( \frac{\theta_i}{z_i} \right)^{1/\alpha} \right] \sum_{i=1}^K \exp \left[ - \left( \frac{\theta_i}{z_i} \right)^{1/\alpha} \right] \\
&\quad + \exp \left[ - \sum_{i=K+1}^n \left( \frac{\theta_i}{z_i} \right)^{1/\alpha} \right] \sum_{1 < i < j \leq K} \left\{ \exp \left[ - \left( \frac{\theta_i}{z_i} \right)^{1/\alpha} - \left( \frac{\theta_j}{z_j} \right)^{1/\alpha} \right] \right\} \\
&\quad + \dots + (-1)^K \exp \left[ - \sum_{i=1}^n \left( \frac{\theta_i}{z_i} \right)^{1/\alpha} \right]
\end{aligned} \tag{15}$$

192 Finally marginalizing over the random effect, we obtain

$$\begin{aligned}
P(Y_1 = y_1, \dots, Y_n = y_n) &= \int G(\mathbf{z}|\mathbf{A})p(\mathbf{A}|\alpha)d\mathbf{A}. \\
&= \int \exp \left[ - \sum_{i=K+1}^n \left( \frac{\theta_i}{z_i} \right)^{1/\alpha} \right] - \exp \left[ - \sum_{i=K+1}^n \left( \frac{\theta_i}{z_i} \right)^{1/\alpha} \right] \sum_{i=1}^K \exp \left[ - \left( \frac{\theta_i}{z_i} \right)^{1/\alpha} \right] \\
&\quad + \exp \left[ - \sum_{i=K+1}^n \left( \frac{\theta_i}{z_i} \right)^{1/\alpha} \right] \sum_{1 < i < j \leq K} \left\{ \exp \left[ - \left( \frac{\theta_i}{z_i} \right)^{1/\alpha} - \left( \frac{\theta_j}{z_j} \right)^{1/\alpha} \right] \right\} \\
&\quad + \dots + (-1)^K \exp \left[ - \sum_{i=1}^n \left( \frac{\theta_i}{z_i} \right)^{1/\alpha} \right] p(\mathbf{A}|\alpha)d\mathbf{A}.
\end{aligned} \tag{16}$$

193 Consider the first term in the summation,

$$\begin{aligned}
\int \exp \left\{ - \sum_{i=K+1}^n \left( \frac{\theta_i}{z_i} \right)^{1/\alpha} \right\} p(\mathbf{A}|\alpha) d\mathbf{A} &= \int \exp \left\{ - \sum_{i=K+1}^n \left( \frac{\left[ \sum_{l=1}^L A_l w_l(\mathbf{s}_i)^{1/\alpha} \right]^\alpha}{z_i} \right)^{1/\alpha} \right\} p(\mathbf{A}|\alpha) d\mathbf{A} \\
&= \int \exp \left\{ - \sum_{i=K+1}^n \sum_{l=1}^L A_l \left( \frac{w_l(\mathbf{s}_i)}{z_i} \right)^{1/\alpha} \right\} p(\mathbf{A}|\alpha) d\mathbf{A} \\
&= \exp \left\{ - \sum_{l=1}^L \left[ \sum_{i=K+1}^n \left( \frac{w_l(\mathbf{s}_i)}{z_i} \right)^{1/\alpha} \right]^\alpha \right\}. \tag{17}
\end{aligned}$$

194 The remaining terms in equation (16) are straightforward to obtain, and after integrating out the random  
195 effect, the joint density for  $K = 0, 1, 2$  is given by

$$P(Y_1 = y_1, \dots, Y_n = y_n) = \begin{cases} G(\mathbf{z}) & K = 0 \\ G(\mathbf{z}_{(1)}) - G(\mathbf{z}) & K = 1 \\ G(\mathbf{z}_{(12)}) - G(\mathbf{z}_{(1)}) - G(\mathbf{z}_{(2)}) + G(\mathbf{z}) & K = 2 \end{cases} \tag{18}$$

196 where

$$G[\mathbf{z}_{(1)}] = P[Z(\mathbf{s}_2) < z(\mathbf{s}_2), \dots, Z(\mathbf{s}_n) < z(\mathbf{s}_n)]$$

$$G[\mathbf{z}_{(2)}] = P[Z(\mathbf{s}_1) < z(\mathbf{s}_1), Z(\mathbf{s}_3) < z(\mathbf{s}_3), \dots, Z(\mathbf{s}_n) < z(\mathbf{s}_n)]$$

$$G[\mathbf{z}_{(12)}] = P[Z(\mathbf{s}_3) < z(\mathbf{s}_3), \dots, Z(\mathbf{s}_n) < z(\mathbf{s}_n)].$$

197 Similar expressions can be derived for all  $K$ , but become cumbersome for large  $K$ .

## 198 References

199 Agresti, A. (2003) *Categorical Data Analysis*. Wiley Series in Probability and Statistics. Wiley, 2nd edn.

- Cohen, J. (1960) A Coefficient of Agreement for Nominal Scales. *Educational and Psychological Measurement*, **20**, 37–46.
- Coles, S. (2001) *An Introduction to Statistical Modeling of Extreme Values*. Lecture Notes in Control and Information Sciences. London: Springer.
- De Oliveira, V. (2000) Bayesian prediction of clipped Gaussian random fields. *Computational Statistics and Data Analysis*, **34**, 299–314.
- Diggle, P. and Ribeiro, P. J. (2007) *Model-based Geostatistics*. Springer Series in Statistics. Springer New York.
- Finley, A. O., Banerjee, S. and Gelfand, A. E. (2015) spBayes for Large Univariate and Multivariate Point-Referenced Spatio-Temporal Data Models. *Journal of Statistical Software*, **63**.
- Genton, M. G., Ma, Y. and Sang, H. (2011) On the likelihood function of Gaussian max-stable processes. *Biometrika*, **98**, 481–488.
- Gneiting, T. and Raftery, A. E. (2007) Strictly Proper Scoring Rules, Prediction, and Estimation. *Journal of the American Statistical Association*, **102**, 359–378.
- de Haan, L. (1984) A Spectral Representation for Max-stable Processes. *The Annals of Probability*, **12**, 1194–1204.
- Heagerty, P. and Lele, S. (1998) A Composite Likelihood Approach to Binary Spatial Data. *Journal of the American Statistical Association*, **1459**, 1099–1111.
- Huser, R. and Davison, A. C. (2014) Space-time modelling of extreme events. *Journal of the Royal Statistical Society: Series B (Statistical Methodology)*, **76**, 439–461.
- Pacifici, K., Reich, B. J., Dorazio, R. M. and Conroy, M. J. (2016) Occupancy estimation for rare species using a spatially-adaptive sampling design. *Methods in Ecology and Evolution*, **7**, 285–293.
- Padoan, S. A., Ribatet, M. and Sisson, S. A. (2010) Likelihood-Based Inference for Max-Stable Processes. *Journal of the American Statistical Association*, **105**, 263–277.
- R Core Team (2016) *R: A Language and Environment for Statistical Computing*. R Foundation for Statistical Computing, Vienna, Austria. URL <https://www.R-project.org/>.
- Reich, B. J. and Shaby, B. A. (2012) A hierarchical max-stable spatial model for extreme precipitation. *The Annals of Applied Statistics*, **6**, 1430–1451.
- Sing, T., Sander, O., Beerenwinkel, N. and Lengauer, T. (2005) ROCr: visualizing classifier performance in R. *Bioinformatics*, **21**, 3940–3941.
- Smith, D. R., Yuancai, L., Walter, C. A. and Young, J. A. (2012) Incorporating predicted species distribution in adaptive and conventional sampling designs. In *Design and Analysis of Long-term Ecological Monitoring Studies* (eds. R. A. Gitzen, J. J. Millspaugh, A. B. Cooper and D. S. Licht), chap. 17, 381–396. Cambridge University Press.
- Stephenson, A. G. (2009) High-Dimensional Parametric Modelling of Multivariate Extreme Events. *Australian & New Zealand Journal of Statistics*, **51**, 77–88.

- 236 Tawn, J. A. (1990) Modelling multivariate extreme value distributions. *Biometrika*, **77**, 245–253.
- 237 Thibaud, E. and Opitz, T. (2015) Efficient inference and simulation for elliptical Pareto processes.  
238 *Biometrika*, **102**, 855–870.
- 239 Wadsworth, J. L. and Tawn, J. A. (2014) Efficient inference for spatial extreme value processes associated  
240 to log-Gaussian random functions. *Biometrika*, **101**, 1–15.
- 241 Wang, X. and Dey, D. K. (2010) Generalized extreme value regression for binary response data: An appli-  
242 cation to B2B electronic payments system adoption. *The Annals of Applied Statistics*, **4**, 2000–2023.